MIMO Interference Alignment in Random Access Networks

Behrang Nosrat-Makouei
Jeffrey G. Andrews and Robert W. Heath, Jr.
Wireless Networking and Communications Group
The University of Texas at Austin, Austin, Texas
Email: {behrang.n.m, jandrews, rheath}@mail.utexas.edu

Radha Krishna Ganti
Department of Electrical Engineering
Indian Institute of Technology Madras
Chennai, India
Email: rganti@ee.iitm.ac.in

***Abstract*—In this paper we analyze a multiple-input-multiple-output interference channel where nodes randomly distributed on a plane utilize interference alignment to reduce the point-to-point outage. We model the spatial distribution of the nodes as a spatial Poisson cluster point process with equal sized clusters. Each cluster uses intra-cluster interference alignment to suppress interference. We link the accuracy of channel state information to the distance between the nodes, i.e., for a fixed SNR, the quality of CSI degrades with increasing distance. Accounting for the inter-cluster unaligned interference, we compare intra-cluster interference alignment with open-loop spatial multiplexing. In our analysis we find common system setups where the benefits of using interference alignment over spatial multiplexing degrade the most due to the imperfect channel state information.**

I. Introduction

Interference alignment (IA) achieves the highest multiplexing gain attainable to date in the K-user multiple-input-multiple-out (MIMO) interference channel [1]. IA confines the interference to a subspace at each receiver such that an interference-free subspace becomes available for the desired signal transmission. Except for *blind* IA techniques [2], [3], which usually attain a lower multiplexing gain, IA requires cooperation between the transmitting/receiving nodes using global channel state information (CSI) [4] or some form of channel reciprocity. In practical scenarios, where CSI is estimated and fed back to the other nodes, the accuracy of the available CSI plays a crucial role in determining the performance of IA [5]. Hence IA is not necessarily the optimal transmission technique in practice. In addition, as the number of available antennas at each node is limited, the number of nodes that can cooperate with each other through IA is also limited [1]. Further, the overheads of cooperative IA grow with the number of users, implying that in many cases it is most efficient to coordinate small groups of users [6]. Consequently it is of interest to investigate the performance of IA networks where a cluster of nodes is cooperating.

Most work on performance of interference alignment is confined to single-cluster performance analysis effectively ignoring the impact of the rest of the network on the distribution of the signal and/or interference (see [5], [7], [8] and references therein). In mobile ad hoc and cellular networks, single cluster analysis does not capture the impact of interference from other nodes in the network which the performance of any PHY/MAC protocol is directly linked to [9]. In [10] the spatial distribution of nodes is considered but the accuracy of the acquired CSI is ignored. This effectively favors IA over transmission techniques which either do not require CSI at the transmitters or are less sensitive to CSI imperfections [5, Section V].

Assuming a fixed transmitter-receiver distance, increasing the density of the nodes decreases the distance between two interfering nodes so fewer resources are consumed for training the cross links. The channel state information at each node therefore becomes more accurate which helps interference alignment inside each cluster. A higher density of the nodes, however, results in more unaligned interference from other clusters and decreases the sum-rate of each cluster. Quantifying this fundamental trade-off is a goal of this paper where we focus on establishing a link between the point-to-point probability of outage, the density of the nodes, the interference at each node, and the effect of varying received power on the accuracy of the estimated CSI for MIMO IA in a clustered ad hoc network. We also compare IA with open-loop spatial multiplexing (SM) to gain further insights into operating regions where employing complicated IA approach is beneficial.

II. System Model

The spatial locations of the nodes, $\mathbf{\Phi}$, are modeled as a planar Newman-Scott cluster point process [11], which is a stationary and isotropic point process with a parent homogeneous poison point process (PPP) of density $\tilde{\lambda}_p$ identifying cluster centers. We assume clusters randomly access the channel with probability P_A effectively reducing the density of this PPP to $\lambda_p = P_A \tilde{\lambda}_p$. Around each cluster center, K transmitters with N antennas each are uniformly distributed in a circle of radius R. The receivers, with N antennas each, are not part of the point process $\mathbf{\Phi}$ and are assumed to be randomly located at distance D_r from each transmitter. Also, the receiver of a transmitter at x is denoted by $\hat{x}$. An instance of the nodes' location is shown

This work was supported by the DARPA IT-MANET program, Grant W911NF-07-1-0028 and the Army Research Labs, Grant W911NF-10-1-0420.

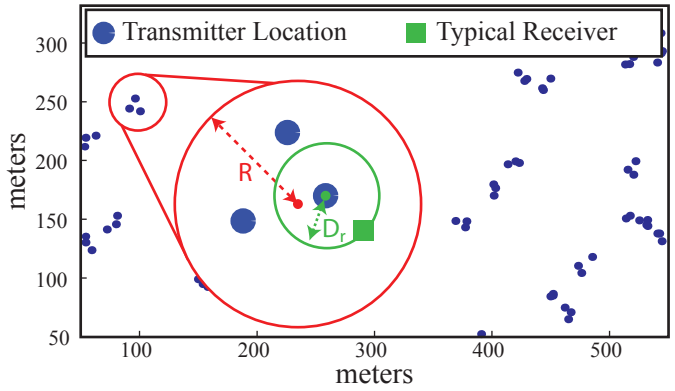

Fig. 1. An instance of the transmitter's distribution with $K = 3$.

in Fig. 1. Consider a typical cluster at the origin, $\mathbf{\Psi}_o$. The received signal at receiver $\hat{x}$, $x \in \mathbf{\Psi}_o$, is

$$\mathbf{y}_{\hat{x}} = \sum_{z \in \mathbf{\Psi}_o} \sqrt{g_{\hat{x}z}} \mathbf{H}_{\hat{x}z} \mathbf{F}_z \tilde{\mathbf{s}}_z + \mathfrak{I}_c + \mathbf{z}_{\hat{x}}, \tag{1}$$

where $\mathfrak{I}_c = \sum_{z \in \mathbf{\Phi}/\mathbf{\Psi}_o} \sqrt{g_{\hat{x}z}} \mathbf{H}_{\hat{x}z} \mathbf{F}_z \tilde{\mathbf{s}}_z$ is the inter-cluster interference, $g_{\hat{x}z}$ and $\mathbf{H}_{\hat{x}z}$ are the pathloss and the matrix of channel coefficients of a block fading channel between the transmitter z and the receiver $\hat{x}$, $\mathbf{F}_z$ is the precoder at transmitter z (we assume $\mathbf{F}_z^* \mathbf{F}_z = \mathbf{I}$) with the transmitted signal $\tilde{\mathbf{s}}_z$ such that $\mathbb{E}\{\tilde{\mathbf{s}}_z^* \tilde{\mathbf{s}}_z\} = P$, and $\mathbf{z}_{\hat{x}} \sim \mathcal{CN}(\mathbf{0}, N_o \mathbf{I})$ is the AWGN. In every cluster, channel state information is estimated at the receivers as in [12] and conveyed to all other nodes of the cluster using an error-free instantaneous feedback link. Thus, the MIMO channels can be modeled as

$$\mathbf{H}_{\hat{x}z} = \sqrt{1 - \beta_{\hat{x}z}^2} \mathbf{H}_{\hat{x}z}^w + \beta_{\hat{x}z} \mathbf{E}_{\hat{x}z} \quad x, z \in \mathbf{\Psi}_o, \tag{2}$$

where $\mathbf{H}_{\hat{x}z}^w$ is the estimated channel, $\mathbf{E}_{\hat{x}z}$ represents the estimation error with i.i.d. terms distributed as $\mathcal{CN}(0,1)$, and $\beta_{\hat{x}z}^2$ is the normalized variance of the estimation error. Assuming a block fading channel model of length T, we set $\beta_{\hat{x}z}$ to be related to the average received SNR at each link, $\gamma_{\hat{x}z}$, as [12, Section II.B]

$$\beta_{\hat{x}z}^2 = \frac{1}{1 + T_t \gamma_{\hat{x}z}} = \frac{1}{1 + T_t \frac{P g_{\hat{x}z}}{N_o}}, \tag{3}$$

where T_t is the number of channel instances spent for training $\mathbf{H}_{\hat{x}z}$. We also assume that $\mathbf{H}^w$ is used to construct the precoders/equalizers and nodes effectively ignore the imperfection in CSI.

III. Intra-cluster Interference Alignment

At each cluster, a K-user system of IA is feasible if there exists a set of matrices $\mathcal{W} = \{\mathbf{W}_{\hat{z}} | z \in \mathbf{\Psi}_0\}$ such that, given the received signal of (1), the following constraints are met [4]

$$\begin{cases} \text{rank}\,(\mathbf{W}_{\hat{x}} \mathbf{H}_{\hat{x}x} \mathbf{F}_x) = N_s \\ \mathbf{W}_{\hat{x}} \mathbf{H}_{\hat{x}z} \mathbf{F}_z = \mathbf{0} \ \forall z \neq x \end{cases} \forall x, z \in \mathbf{\Psi}_o, \tag{4}$$

where $\mathbf{W}_{\hat{x}}$ is the combining filter used at receiver $\hat{x}$ and N_s is the number of interference-free streams each transmitter can send to its receiver. The linear equalizer presented in [5] and the projection matrix presented in [13, Section III.A] are examples of a possible receive filter in (4). We assume the set of $\{N, N_s, K\}$ constitutes a feasible IA system [14].

A. Characterizing the SINR

From (4), interference at receiver $\hat{x}$ is confined to an $N - N_s$ dimensional subspace. Let $[\{\cdot\}]$ represent horizontal concatenation of the elements in $\{\cdot\}$. Then, as IA precoders/equalizers are constructed using $\mathbf{H}^w$ as given by (2), the $N \times (K-1)N_s$ matrix of $\mathbf{J}_{\hat{x}} = [\{\mathbf{H}_{\hat{x}z}^w \mathbf{F}_z | z \neq x, z \in \mathbf{\Psi}_o\}]$ spans an $N - N_s$ dimensional subspace. Let the singular value decomposition of $\mathbf{J}_{\hat{x}}$ be $\mathbf{U}_{\mathbf{J}_{\hat{x}}} \mathbf{\Sigma}_{\mathbf{J}_{\hat{x}}} \mathbf{V}_{\mathbf{J}_{\hat{x}}}^*$ and let the rows of $\mathbf{W}_{\hat{x}}$ be the columns of $\mathbf{U}_{\mathbf{J}_{\hat{x}}}$ corresponding to zero singular values in $\mathbf{\Sigma}_{\mathbf{J}_{\hat{x}}}$. As $\mathbf{W}_{\hat{x}}$ is independent of $\mathbf{H}_{\hat{x}x}^w \mathbf{F}_x$, it satisfies the conditions in (4) and is a valid zero-forcing (ZF) equalizer for IA. Using this ZF receiver, the post processing SINR of the nth stream at receiver $\hat{x}$ is

$$\gamma_{\hat{x},n}^{\text{IA}} = \frac{g_{\hat{x}x}(1 - \beta_{\hat{x}x}^2) \tilde{\mathbf{h}}_{\hat{x}x}^* \tilde{\mathbf{h}}_{\hat{x}x}}{\frac{N_s N_o}{P} + \underbrace{\sum_{z \in \mathbf{\Psi}_o} g_{\hat{x}z} \beta_{\hat{x}z}^2 \tilde{\mathbf{e}}_{\hat{x}z}^* \tilde{\mathbf{e}}_{\hat{x}z}}_{I_e} + \underbrace{\sum_{z \in \mathbf{\Phi}/\mathbf{\Psi}_o} g_{\hat{x}z} \tilde{\mathbf{h}}_{\hat{x}z}^* \tilde{\mathbf{h}}_{\hat{x}z}}_{I_i}}, \tag{5}$$

where for all $z \in \mathbf{\Phi}$, $\tilde{\mathbf{h}}_{\hat{x}z} = (\mathbf{e}_n^* \mathbf{W}_{\hat{x}} \mathbf{H}_{\hat{x}z}^w \mathbf{F}_z)^*$ and $\tilde{\mathbf{e}}_{\hat{x}z} = (\mathbf{e}_n^* \mathbf{W}_{\hat{x}} \mathbf{E}_{\hat{x}z} \mathbf{F}_z)^*$, and $\mathbf{e}_n$ is the nth column of an $N_s \times N_s$ identity matrix. Let entries of $\mathbf{H}_{\hat{x}z}$ and $\mathbf{E}_{\hat{x}z}$ be i.i.d. Gaussian terms. Due to the doubly unitarily invariance of the Gaussian distribution, $\tilde{\mathbf{h}}_{\hat{x}z}$ and $\tilde{\mathbf{e}}_{\hat{x}z}$ will be column vectors of length N_s with i.i.d. Gaussian terms.

B. Probability of Outage

In (5), as $\tilde{\mathbf{h}}_{\hat{x}z}^* \tilde{\mathbf{h}}_{\hat{x}z}$ and $\tilde{\mathbf{e}}_{\hat{x}z}^* \tilde{\mathbf{e}}_{\hat{x}z}$ are i.i.d. $\Gamma(N_s, 1)$ random variables, we denote them by $h_{\hat{x}z}$ for notational simplicity. Let the transmitter corresponding the typical receiver be at the origin and denote it by o. The probability of success is

$$\mathrm{P}_{\mathrm{s}}^{\mathrm{IA}}(\theta) = \mathbb{P}^{!\mathrm{o}}(\mathtt{SINR}(\mathrm{o}, \hat{\mathrm{o}}) > \theta), \tag{6}$$

where $\mathbb{P}^{!o}$ represents the reduced Palm probability measure and θ is the SINR threshold. Theorem 1 gives a closed-form expression of (6) when nodes of each cluster cooperate through IA.

Theorem 1. *For the system model described in Section II, the success probability with IA equals*

$$\mathrm{P}_{\mathrm{s}}^{\mathrm{IA}}(\theta) = \sum_{\mathrm{k}=0}^{\mathrm{N_s}-1} \frac{(-\eta)^{\mathrm{k}}}{\mathrm{k!}} \frac{\mathrm{d}^{\mathrm{k}}}{\mathrm{ds}^{\mathrm{k}}} \mathrm{e}^{-\mathrm{s}\frac{\mathrm{N_s N_o}}{\mathrm{P}}} \mathcal{L}_{\mathrm{I_e}}^{!\mathrm{o}}(\mathrm{s}) \mathcal{L}_{\mathrm{I_i}}(\mathrm{s}) \Big|_{\mathrm{s}=\eta}, \tag{7}$$

where $\mathcal{L}_{\mathrm{I_e}}^{!o}(s)$ and $\mathcal{L}_{\mathrm{I}_i}(s)$ are given in (11) *and* (13) *respectively, and $\eta = \frac{\theta}{g_{\hat{o}o}(1 - \beta_{\hat{o}o}^2)}$.*

Proof: Since $h_{\hat{o}o} \sim \Gamma(N_s, 1)$, its complementary cumulative distribution function (CCDF) is $F(x) = \frac{\Gamma(N_s, x)}{\Gamma(N_s)} =$

$e^{-x}\sum_{k=0}^{N_s-1}\frac{x^k}{k!}$. Hence, as I_e and I_i in (5) are independent, (6) equals

$$\mathrm{P_s^{IA}} = \sum_{k=0}^{N_s-1}\frac{\eta^k}{k!}\mathbb{E}^{!0}\left[\left(\frac{N_sN_o}{P}+I_e+I_i\right)^k e^{-\eta\left(\frac{N_sN_o}{P}+I_e+I_i\right)}\right],$$
$$\overset{(a)}{=} \sum_{k=0}^{N_s-1}\frac{(-\eta)^k}{k!}\frac{\mathrm{d}^k}{\mathrm{d}s^k}\mathbb{E}^{!o}e^{-s\left(\frac{N_sN_o}{P}+I_e+I_i\right)}\Big|_{s=\eta},$$

where (a) follows from the properties of the Laplace transform. The reduced Palm probability of a Newman-Scott cluster process is $\mathbb{P}^{!o}=\mathbb{P}*C^{!o}$ where $*$ denotes superposition [11]. This implies that assuming a point of the cluster process at the origin equals the original point process $\mathbf{\Phi}$ and an additional cluster which has a point at the origin. Also this additional cluster at the origin is independent of the original process $\mathbf{\Phi}$ and we represent this cluster by $\mathbf{\Psi}_o$. So we have

$$\mathrm{P_s^{IA}} = \sum_{\mathrm{k=0}}^{\mathrm{N_s-1}}\frac{(-\eta)^{\mathrm{k}}}{\mathrm{k!}}\frac{\mathrm{d^k}}{\mathrm{ds^k}}\mathrm{e}^{-\mathrm{s}\frac{\mathrm{N_sN_o}}{\mathrm{P}}}\mathbb{E}\mathrm{e}^{-\mathrm{sg_{\hat{o}o}}\beta_{\hat{o}o}^2\mathrm{h_{\hat{o}o}}}\mathcal{L}_{\mathrm{I_e}}^{!\mathrm{o}}(\mathrm{s})\mathcal{L}_{\mathrm{I_i}}(\mathrm{s})\Big|_{\mathrm{s}=\eta},$$

where $\mathcal{L}_{\mathrm{I}_e}^{!o}(s)$ is the Laplace transform of the intra-cluster interference with respect to the reduced Palm measure and $\mathcal{L}_{\mathrm{I}_i}(s)$ is the Laplace transform of the inter-cluster interference. Since $h_{\hat{o}o}$ is exponentially distributed, using (3),

$$\mathbb{E}e^{-sg_{\hat{o}o}\beta_{\hat{o}o}^2h_{\hat{o}o}} = \frac{\frac{T_tP}{N_o}+D_r^\alpha}{s+\frac{T_tP}{N_o}+D_r^\alpha}. \tag{8}$$

We now evaluate $\mathcal{L}_{\mathrm{I}_e}^{!o}(s)$

$$\mathcal{L}_{\mathrm{I}_e}^{!o}(s) = \mathbb{E}^{!o}\left[e^{-s\sum\limits_{z\in\mathbf{\Psi}_o}g_{\hat{o}z}\beta_{\hat{o}z}^2h_{\hat{o}z}}\right]$$
$$= \mathbb{E}^{!o}\left[\prod_{z\in\mathbf{\Psi}_o}e^{-sg_{\hat{o}z}\beta_{\hat{o}z}^2h_{\hat{o}z}}\right]$$
$$= \mathbb{E}^{!o}\left[\prod_{z\in\mathbf{\Psi}_o}\left(\frac{1}{1+sg_{\hat{o}z}\beta_{\hat{o}z}^2}\right)^{N_s}\right] \tag{9}$$
$$= \mathbb{E}^{!o}\left[\prod_{z\in\mathbf{\Psi}_o}\left(\frac{\frac{T_tP}{N_o}+\|z-\hat{o}\|^\alpha}{s+\frac{T_tP}{N_o}+\|z-\hat{o}\|^\alpha}\right)^{N_s}\right]. \tag{10}$$

To derive (9) the Laplace transform of $h_{\hat{o}z}$ was used and in the last step we have substituted $\|x\|^{-\alpha}$ for the path loss. Observe that (10) is the probability generating functional of the representative cluster $\mathbf{\Psi}_o$ with respect to its reduced Palm probability. We use the following result from [15, Lemma 1] which we state for completeness. For any function $f(x):\mathbb{R}^2\to\mathbb{R}^+$,

$$\mathbb{E}^{!o}\prod_{x\in\mathbf{\Psi}_o}f(x) = \frac{1}{\pi R^2}\int_A\left(\frac{1}{\pi R^2}\int_A f(x-y)\mathrm{d}x\right)^{K-1}\mathrm{d}y,$$

where $A=B(o,R)$. Using the above result, we obtain

$$\mathcal{L}_{\mathrm{I}_e}^{!o}(s) = \int_{B(o,R)}\left[\frac{1}{\pi R^2}\int_{B(o,R)}\left(\frac{\frac{T_tP}{N_o}+\|x-y-\hat{o}\|^\alpha}{s+\frac{T_tP}{N_o}+\|x-y-\hat{o}\|^\alpha}\right)^{N_s}\mathrm{d}x\right]^{K-1}\mathrm{d}y. \tag{11}$$

We now focus on $\mathcal{L}_{\mathrm{I}_i}(s)$

$$\mathcal{L}_{\mathrm{I}_i}(s) = \mathbb{E}^{!o}\left[e^{-s\sum_{z\in\mathbf{\Phi}}g_{\hat{o}z}h_{\hat{o}z}}\right]$$
$$= \mathbb{E}^{!o}\left[\prod_{z\in\mathbf{\Phi}}\left(\frac{1}{1+s\|x-\hat{o}\|^{-\alpha}}\right)^{N_s}\right]. \tag{12}$$

To calculate (12), we use the following result which characterizes the probability generating functional of a Poisson cluster process [11]

$$\mathbb{E}\prod_{x\in\mathbf{\Phi}}f(x) = \exp\left(-\lambda_p\int_{\mathbb{R}^2}1-\left(\frac{1}{\pi R^2}\int_{B(o,R)}f(x-y)\mathrm{d}x\right)^K\mathrm{d}y\right).$$

Using the above probability generating functional, we obtain

$$\mathcal{L}_{\mathrm{I}_i}(s) = \exp\left(-\lambda_p\int_{\mathbb{R}^2}1-\left[\frac{1}{\pi R^2}\int_{B(o,R)}\left(\frac{\|x-y\|^\alpha}{s+\|x-y\|^\alpha}\right)^{N_s}\mathrm{d}x\right]^K\mathrm{d}y\right). \tag{13}$$

■

IV. Spatial Multiplexing

An alternative strategy to interference alignment is spatial multiplexing where the channels are time-shared with TDMA. We analyze open-loop spatial multiplexing where at each cluster only a single transmit/receiver pair communicate N streams without precoding. Following (2), the received signal at a typical receiver can be written as

$$\mathbf{y}_{\hat{x}} = g_{\hat{x}x}\left(\sqrt{(1-\beta_{\hat{x}x}^2)g_{\hat{x}x}}\mathbf{H}_{\hat{x}x}^w+\beta_{\hat{x}x}\mathbf{E}_{\hat{x}x}\right)\tilde{\mathbf{s}}_x+\mathfrak{I}_c+\mathbf{z}_{\hat{x}},$$

where $\mathfrak{I}_c$ is defined in (1) with the difference that each cluster only has a single transmitter. In this case, the point process of the transmitters simplifies to the Poisson point process of the parent points. When $\beta_{\hat{x}x}=0$, after a zero-forcing receiver based on $\mathbf{H}_{\hat{x}x}$, SINR of the nth stream at a typical receiver can be written as

$$\gamma_{\hat{x},n}^{\mathrm{SM}} = \frac{g_{\hat{x}x}}{\mathbf{e}_n^*(\mathbf{H}_{\hat{x}x}^w)^{-1}\left(\frac{NN_o}{P}+\sum\limits_{z\in\mathbf{\Phi}/\mathbf{\Psi}_o}g_{\hat{x}z}\mathbf{H}_{\hat{x}z}\mathbf{H}_{\hat{x}z}^*\right)(\mathbf{H}_{\hat{x}x}^w)^{-*}\mathbf{e}_n}, \tag{14}$$

where we have assumed the interference channels from different transmitters are independent. The probability of success in this case is given by [16]

$$\mathrm{P_s^{SM}}(\theta) = \mathbb{P}^{!o}(\gamma_{\hat{x},n}^{\mathrm{SM}}>\theta)$$
$$= \exp\left(-\lambda_p\theta^{\frac{2}{\alpha}}D_r^2\mathcal{J}-\theta D_r^\alpha\frac{NN_o}{P}\right), \tag{15}$$

where $\mathcal{J}=\frac{\pi\Gamma\left(N+\frac{2}{\alpha}\right)\Gamma\left(1-\frac{2}{\alpha}\right)}{\Gamma(N)}$. With imperfect CSI, we assume the receivers compute their zero-forcing receivers based on the estimated channel values and ignore the estimation error. Then, the denominator of (14) will have an additional term of $g_{\hat{x}x}\beta_{\hat{x}x}^2\mathbf{E}_{\hat{x}x}\mathbf{E}_{\hat{x}x}^*$ inside the parenthesis. As the channel estimation error is independent of the estimated channel and the transmitter/receiver distance is fixed to D_r, this additional term is effectively increasing the noise spectral density from

N_o to $N_o + Pg_{\hat{x}x}\beta_{\hat{x}x}^2$. As the numerator of (14) also changes to $g_{\hat{x}x}\left(1-\beta_{\hat{x}x}^2\right)$, in case of imperfect CSI as in (2), the probability of success at a typical receiver for any of the streams changes from (15) to

$$\begin{aligned} \mathrm{P}_{\mathrm{s}}^{\mathrm{SM}}(\theta) &= \mathbb{P}^{!o}(\gamma_{\hat{x},n}^{\mathrm{SM}} > \theta) \\ &= \exp\left(-\lambda_p \tilde{\theta}^{\frac{2}{\alpha}} D_r^2 \vartheta - \tilde{\theta} D_r^{\alpha} \frac{N\tilde{N}_o}{P}\right), \end{aligned} \tag{16}$$

where $\tilde{\theta} = \frac{\theta}{1-\beta_{\hat{x}x}^2}$ and $\tilde{N}_o = N_o + Pg_{\hat{x}x}\beta_{\hat{x}x}^2$.

V. Simulation

In this section, for simplicity, we focus on the case of $K=3$, $N=2$, and $N_s=1$. To further reduce the number of involved variables, we set R to $D_c=0.5\lambda_p^{0.5}$ (average distance between the cluster centers) and set D_r to $\frac{R}{5}$. In this way, by increasing D_c, all the nodes move away from each other. We set N_o to 1 and $\frac{P}{N_o}$ to 30dB. We also assume all the clusters are transmitting simultaneously. In the forthcoming discussions, perfect channel estimation corresponds to very large values of the training period, T_t, where β is assumed to be 0 and the worst channel estimation corresponds to assigning the least number of channel instances for training. i.e. $T_t = N = 2$. Note that for perfect CSI, (8) and (11) are both equal to 1.

Assume perfect channel state information. The probability of successful transmission given by (7) as a function of average distance between the cluster centers and varying SINR thresholds is shown in Fig. 2. It appears that when probability of successful transmission is the metric of interest, IA can be utilized for dense and moderately dense networks. The important question, however, is whether using a much more simpler transmission techniques, such as open loop spatial multiplexing, could yield to a better (or comparative) performance. Using (7) and (15), the difference between the probability of successful transmission of IA and SM ($\mathrm{P}_{\mathrm{s}}^{\mathrm{IA}} - \mathrm{P}_{\mathrm{s}}^{\mathrm{SM}}$) is shown in Fig. 3. As can be seen, for very dense networks, SM outperforms IA which can be explained by the reduced inter-cluster interference due to only a single transmit/receiver pair being active at each cluster. In addition, for moderately dense networks, IA outperforms SM.

Now assume $T_t = N = 2$ where the channel estimation errors have the highest variance. The questions of interest are i)how much the performance of IA will be affected by introducing the imperfect CSI and ii)how does the relative performance between IA and SM change in this scenario. For the same range of D_c and θ as the previous plots, the decrease in the probability of successful transmission for IA when the training period is lowered to 2 is shown in Fig. 4. Probability of successful transmission for IA remains unchanged for dense networks but is reduced for moderate node densities. Using (7) and (16), $\mathrm{P}_{\mathrm{s}}^{\mathrm{IA}} - \mathrm{P}_{\mathrm{s}}^{\mathrm{SM}}$ is also shown in Fig. 5 where, as expected, SM has a better performance even for a larger range of the node densities and, as hinted by Fig. 4, IA has lost most of its privileges at moderate node densities. As a reference, the accuracy of (7) when $T_t = 2$, as obtained through comparing

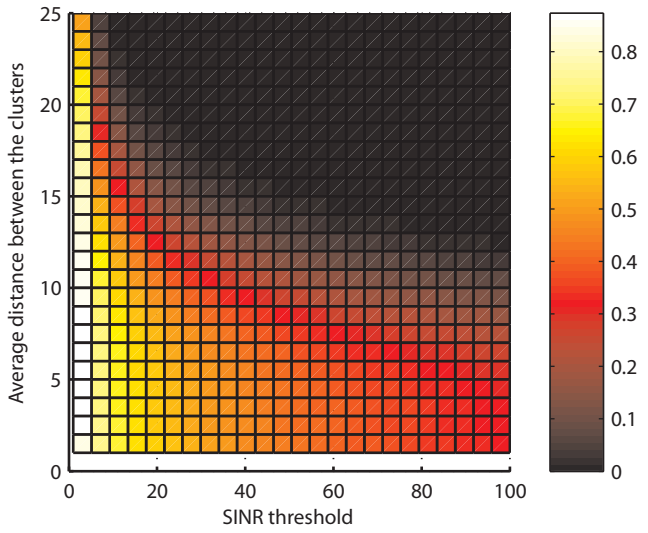

Fig. 2. Probability of successful transmission for IA as a function of the average distance between the cluster centers and the SINR threshold with perfect CSI.

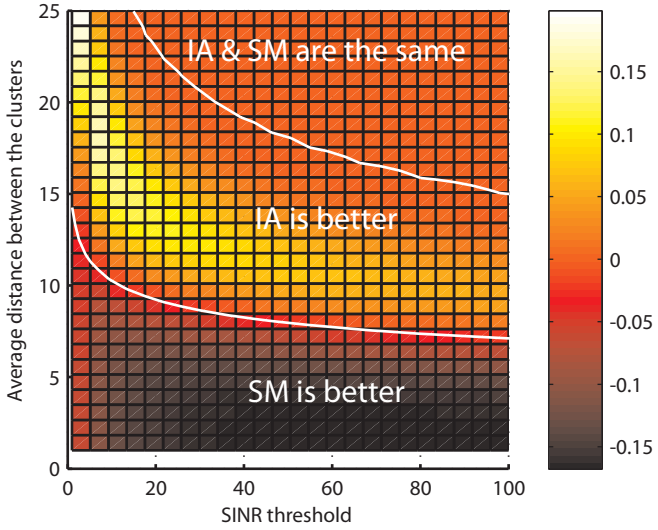

Fig. 3. Difference between the probability of successful transmission of IA and SM, $\mathrm{P}_{\mathrm{s}}^{\mathrm{IA}} - \mathrm{P}_{\mathrm{s}}^{\mathrm{SM}}$, as a function of the average distance between cluster centers and the SINR threshold for perfect CSI.

with numerical results, is shown in Fig. 6 where the worst case error is less than 0.0035.

VI. Conclusion

We obtained an expression for the probability of successful transmission in a clustered MIMO IA network when the impact of channel estimation on the accuracy of the obtained CSI is taken into account. The probability of successful transmission for IA and SM was compared for a wide range of variables and we showed that SM can outperform IA in high node densities. We also showed that when imperfect CSI is taken into account, the range of parameters where SM outperforms IA expands. We leave a more thorough analysis of performance differences

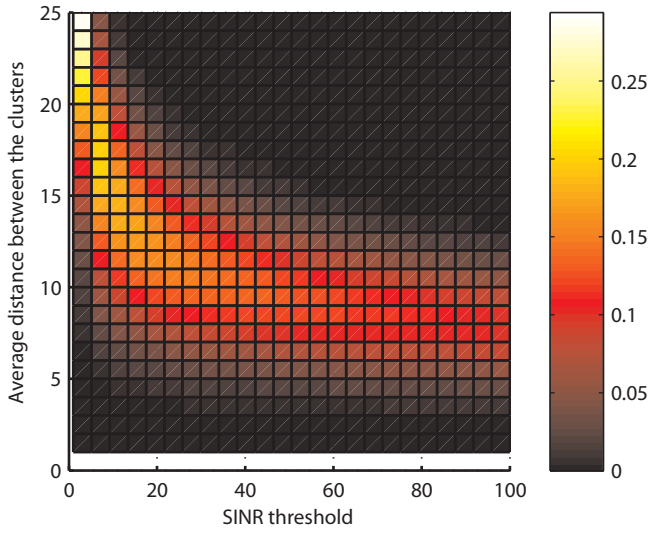

Fig. 4. $\mathrm{P_s^{IA}}|_{\mathrm{T_t}\to\infty} - \mathrm{P_s^{IA}}|_{\mathrm{T_t}=2}$ showing how much the probability of successful transmission for IA can reduce as a result of reducing the training period.

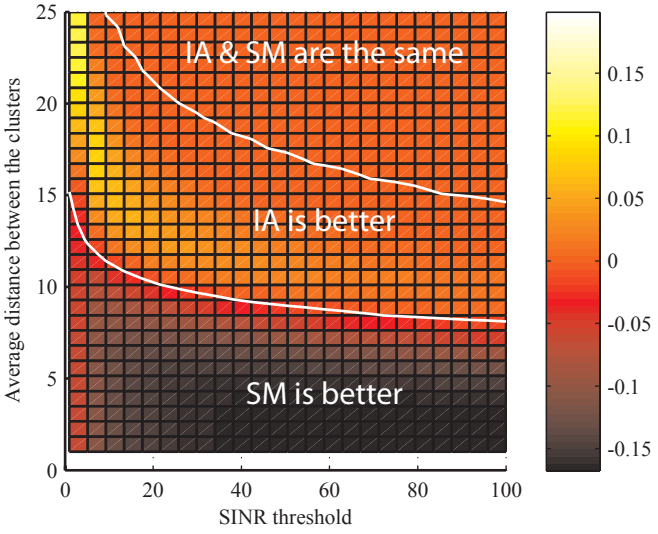

Fig. 5. Difference between the probability of successful transmission of IA and SM, $\mathrm{P_s^{IA}} - \mathrm{P_s^{SM}}$, as a function of the average distance between cluster centers and the SINR threshold for the worst channel estimation error variance ($T_t = 2$).

between IA and SM, especially when network wide objective functions such as transmission capacity are involved, for future work. We fixed the channel training period and the channel access probability; future work will consider the optimization of these parameters.

REFERENCES

[1] T. Gou and S. A. Jafar, "Degrees of freedom of the K user $MtimesN$ MIMO interference channel," *IEEE Trans. Inf. Theory*, vol. 56, no. 12, pp. 6040–6057, Dec. 2010.

[2] S. A. Jafar, "Exploiting channel correlations - simple interference alignment schemes with no CSIT," in *Proc. IEEE Global Telecommun. Conf.*, Miami, FL, Dec. 2010, pp. 1–5.

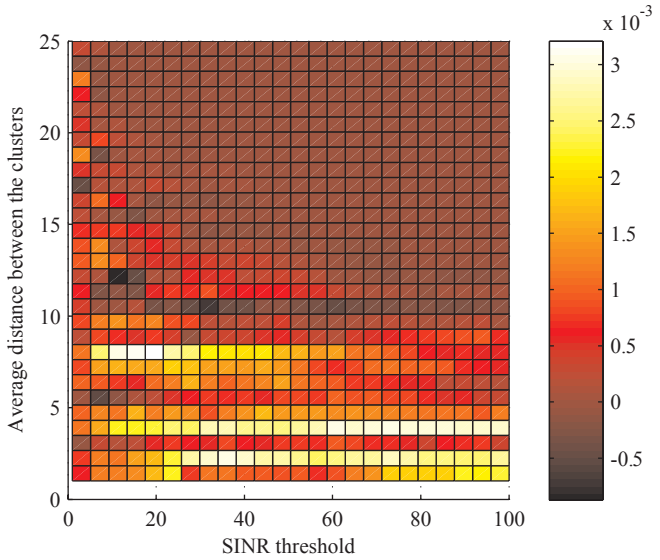

Fig. 6. Accuracy of $\mathrm{P_s^{IA}}$ as given by (7) for the worst channel estimation error variance.

[3] T. Gou, C. Wang, and S. A. Jafar, "Aiming perfectly in the dark - blind interference alignment through staggered antenna switching," *IEEE Trans. Signal Process.*, vol. 59, no. 6, pp. 2734–2744, June 2011.

[4] V. Cadambe and S. Jafar, "Interference alignment and degrees of freedom of the K-user interference channel," *IEEE Trans. Inf. Theory*, vol. 54, no. 8, pp. 3425–3441, Aug. 2008.

[5] B. Nosrat-Makouei, J. G. Andrews, and R. W. Heath, Jr., "MIMO interference alignment over correlated channels with imperfect CSI," *IEEE Trans. Signal Process.*, vol. 59, no. 6, pp. 2783 – 2794, June 2011.

[6] S. W. Peters and R. W. Heath, Jr., "Orthogonalization to reduce overhead in MIMO interference channels," in *Proc. Int. Zurich Seminar on Commun.*, Zurich, Switzerland, Mar. 2010, pp. 126–129.

[7] O. El Ayach and R. W. Heath, Jr., "Interference alignment with analog channel state feedback," to appear in *IEEE Trans. Wireless Commun.*, preprint available online at arXiv:1010.2787v3, Nov. 2011.

[8] B. Nosrat-Makouei, J. G. Andrews, and R. W. Heath, "User arrival in MIMO interference alignment networks," to appear in *IEEE Trans. Wireless Commun.*, preprint available online at arXiv:1106.5253v1, June 2011.

[9] F. Baccelli and B. Blaszczyszyn, *Stochastic Geometry and Wireless Networks, Part II: Applications*. Now Publishers, 2009.

[10] R. Tresch, G. Alfano, and M. Guillaud, "Interference alignment in clustered ad hoc networks: High reliability regime and per-cluster Aloha," in *Proc. IEEE Int. Conf. Acoust. Spch. Signal Process.*, Prague, Czech Republic, May 2011, pp. 3348–3351.

[11] D. Stoyan, W. Kendall, and J. Mecke, *Stochastic Geometry and Its Applications*, ser. Wiley-interscience paperback series. John Wiley & Sons, 2008.

[12] G. Caire, N. Jindal, M. Kobayashi, and N. Ravindran, "Multiuser MIMO achievable rates with downlink training and channel state feedback," *IEEE Trans. Inf. Theory*, vol. 56, no. 6, pp. 2845–2866, June 2010.

[13] S. W. Peters and R. W. Heath, "Cooperative algorithms for MIMO interference channels," *IEEE Trans. Veh. Technol.*, vol. 60, no. 1, pp. 206–218, Jan. 2011.

[14] C. Yetis, T. Gou, S. Jafar, and A. Kayran, "On feasibility of interference alignment in MIMO interference networks," *IEEE Trans. Signal Process.*, vol. 58, no. 9, pp. 4771–4782, Sept. 2010.

[15] R. K. Ganti and M. Haenggi, "Interference and outage in clustered wireless ad hoc networks," *IEEE Trans. Inf. Theory*, vol. 55, no. 9, pp. 4067–4086, Sept. 2009.

[16] R. H. Y. Louie, M. R. McKay, and I. B. Collings, "Open-loop spatial multiplexing and diversity communications in ad hoc networks ," *IEEE Trans. Inf. Theory*, vol. 57, no. 1, pp. 317–344, Jan. 2011.